Published in: Superconductor Science & Technology (1998), vol.11, iss.1, pp.94-100
Status: Postprint (Author's version)

Magnetic flux penetration and creep in BSSCO-2223 composite ceramics

Ph Vanderbemden†, Ch Destombes†, R Cloots‡ and M Ausloos§

† *SUPRAS, Montefiore Electricity Institute B28, University of Liège, Sart-Tilman, B-4000 Liège, Belgium*
‡ *SUPRAS, Chemistry Institute B6, University of Liège, Sart-Tilman, B-4000 Liège, Belgium*
§ *SUPRAS Physics Institute B5, University of Liège, Sart-Tilman, B-4000 Liège, Belgium*

Abstract. We have experimentally investigated the magnetic flux penetration through a Bi-2223 polycrystalline superconductor synthesized by a classical solid-state reaction method. Electrical resistance, AC susceptibility, the Campbell method and magnetic flux waveform recordings have been analysed and compared in order to separate clearly intergrain and intragrain contributions. The AC susceptibility frequency dependence has been also examined at T = 77 K in a broad field range (0.01 G< B_{AC} < 100 G). The activation energy as a function of AC applied magnetic field is found to present a pronounced minimum for an induction (8 G) corresponding to full magnetic flux penetration through the intergranular matrix.

1. Introduction

The magnetic behaviour of bulk polycrystalline high-T_c superconductors is quite difficult to predict since they present a very complex and disordered microstructure. That is probably the reason why so many experiments are performed on these granular materials. Generally speaking, two supercurrent paths are present in the sample. In addition to intragranular currents screening individual superconducting grains, intergranular currents are flowing through weak links connecting neighbouring grains [1]. The corresponding intergranular current density is several orders of magnitude smaller than the intragranular one and is very sensitive to low magnetic fields [2,3]. If the intragranular current behaviour is a fundamental quantity for theoretical understanding, knowledge of the intergranular one is markedly necessary for practical purposes. As a consequence, we need to characterize the coupling between grains in order to understand the magnetic and transport properties of these ceramics.

Nowadays, there are still ambiguities in the determination of critical currents obtained by different measuring methods [4]. For example, the critical current density J_c determined by DC magnetization measurement is found to be a kind of average of the transport critical current density and the intragranular current density [5]. Flux creep and flux flow effects alter critical current measurements as well. Hence J_c usually depends on the time scale of the specific experimental technique used for its determination. Some authors [6] also argue that the reversible motion of flux lines significantly affects the magnetic properties, giving rise to an analysis overestimating the local critical current density.

The purpose of this communication is to present and compare a set of different magnetic and electrical measurements performed on polycrystalline BSCCO-2223 materials. The measured transport critical current value of the present samples is rather small (50 A cm^{-2} at T = 77 K and H = 0), owing to the fact that the material is a non-textured polycrystalline ceramic. Nevertheless, the value of the full penetration induction B^* will be found to be 8 G at T = 77 K. This implies that we have experimentally the ability to explore the characteristics of the flux penetration in a broad field range, from $B << B^*$ to $B >> B^*$, and to report interesting findings.

This paper is organized as follows: in section 2, the ceramic synthesis method is briefly described together with measurement experimental details. Section 3 is devoted to the presentation and discussion of the results. In section 4 frequency and field dependences of the real part of the AC susceptibility (χ') are discussed within a flux creep model. Finally, conclusions are the subject of section 5.

2. Experimental techniques

2.1. Synthesis process and microstructural characterization

The $Bi_2Sr_2Ca_2Cu_3O_{10}$ material, subsequently called the 2223 sample, analysed below has been synthesized by using a classical solid-state reaction method. High-purity powders of Bi_2O_3, $SrCO_3$, $CaCO_3$ and CuO were mixed very homogeneously, ground and then progressively heated to 850 °C in an alumina crucible. This temperature was maintained for 144 h with two intermediary grindings at room temperature at regular intervals. The SEM

observation (figure 1) reveals a large porosity of the 2223 sample. The superconducting 2223 grains look like small needles with length between 10 and 30 μm and diameter ca 1 μm. An energy-dispersive x-ray analysis performed of the surface of a polished sample indicates that the secondary phases have mostly a chemical composition close to the 2212 stoichiometry, i.e. are made of $Bi_2Sr_2CaCu_2O_8$.

Figure 1: *Scanning electron micrograph of a polished section of the BSSCO-2223 ceramic material prepared as described in the text.*

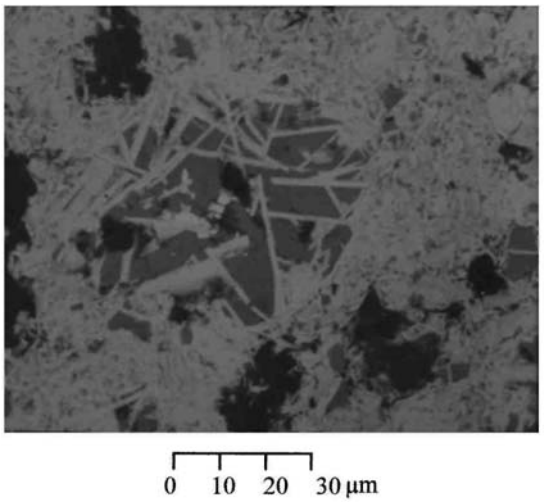

Figure 2: *Geometry of the sample used for magnetic measurements.*

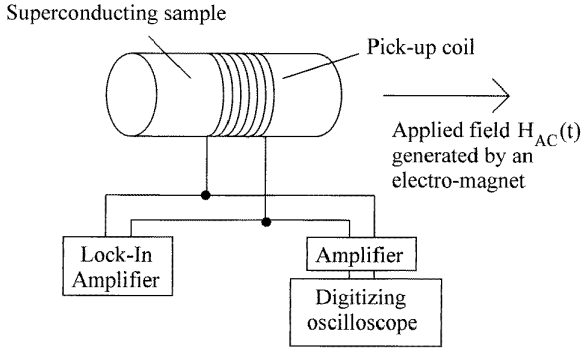

2.2. Magnetic properties

The sample which was studied was cut as a long cylinder from the polycrystalline pellet (figure 2). The cross-section is 3 mm^2 and the length is 12 mm. In order to avoid complicating demagnetization effects, the direction of the magnetic field has always been applied parallel to the long axis of the cylinder. Magnetic properties have been measured in a home-made susceptometer based on a CTI-8001 cryocooler. Great care has been taken to eliminate Foucault currents in the vicinity of the sample. The sinusoidal magnetic field is generated by an electromagnet, made up of a sheeted iron core and four generating coils driven by an HP8904A synthesizer followed by a C-audio ST600 power amplifier. The sample response is then measured with a pick-up coil made of fine copper wire (50 μm diameter) tightly wrapped in the central part of the cylinder (figure 2). The real and the imaginary parts of the AC magnetic susceptibility are measured by using a EGG5210 lock-in amplifier, whereas we use a HP54503A digitizing oscilloscope for magnetic flux waveform recording.

When investigating the frequency dependence (100 Hz-10 kHz) of the magnetic properties it is imperative to make sure that AC field amplitude remains constant. This requires a careful calibration procedure. In our experiments, the field stability has been checked to be better than 0.1%. Furthermore, our experimental system used for susceptibility determination is just made up of a single sensing coil (figure 2); as a consequence no circuit resonances of the measuring system will disturb the signal.

Figure 3: *Principle of the transport critical current determination.*

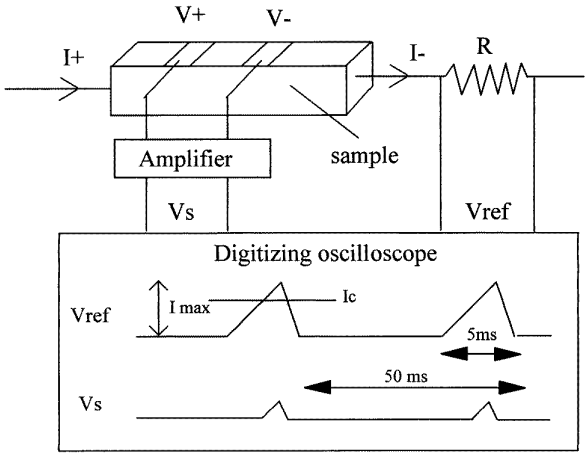

2.3. Transport critical current

A classical four-point method has been used to determine the transport critical current at T = 77 K. Electrical contacts are made of indium paste. In order to avoid spurious heating due to the contact resistances, the whole system is immersed in a liquid nitrogen bath and the driving current has the form of short periodic triangular pulses (figure 3). The voltage drop across the sample is then amplified and applied to a digitizing oscilloscope. The critical current J_c is determined by taking 1 μV cm^{-1} as the electrical field threshold.

2.4. Electrical resistance

Electrical resistance data have been obtained following an automated sequence and acquisition scheme [7]. The classical four-point method is used, carrying a current density of the order of 0.1 A cm^{-2}. The potential difference is measured with a Keithley 181 nanovoltmeter.

3. Results and discussion

3.1. Electrical resistivity and AC magnetic susceptibility

Figure 4 shows the temperature dependence of both electrical resistivity and AC magnetic susceptibility ($\mu_0 h_{AC}$ = 1 G, f = 1053 Hz). The initial drop of resistivity, marking the influence of the superconducting fluctuations, occurs noticeably at $T \approx 115$ K. The ρ versus T curve exhibits a 'resistive-tail' shape (a signature of the granular microstructure) and vanishes at T = 100 K. The temperature derivative of $\rho(T)$ has been numerically determined and is shown in figure 4. The main peak at 109 K characterizes the Ginzburg-Landau temperature and the intragrain transition width is ca 4 K. The second peak at a lower temperature is rather sharp and indicates that the inhomogeneous weak links are not too dispersed in chemical content [8].

On the other hand, the susceptibility results display a small intragranular shielding, clearly visible in the temperature range 101 K-109 K through the smooth decay of χ'. These shielding currents are reversible ($\chi'' = 0$) in that temperature range, suggesting that no vortices are penetrating the grains, i.e. $H < H_{C1g}$ where H_{C1g} is the lower critical field of the grains. However, H_{C1g} vanishes at $T = T_c$ and we might expect a narrow ΔT range in the vicinity of T_c where $H_{C1g}(T) < H$ and $\chi'' > 0$. An explanation is that the penetration depth near T_c is probably larger than the small grain diameter (1 μm), so that there is no vortex (mixed state) in the grains [1]. The susceptibility onset occurs at the 2223 phase critical temperature (109.5 K), which corresponds to the inflection point in the $\rho(T)$ curve (upper maximum of dρ/dT). It clearly appears that the intergranular shielding becomes really efficient below the zero-resistivity temperature (100 K), when a percolation path is well established throughout the sample [9,10].

Published in: Superconductor Science & Technology (1998), vol.11, iss.1, pp.94-100
Status: Postprint (Author's version)

Figure 4: *Electrical resistivity ρ (●), dρ/dT (○) and AC susceptibility measurements as a function of temperature.* B_{AC} *= 1 G, f= 1053 Hz.*

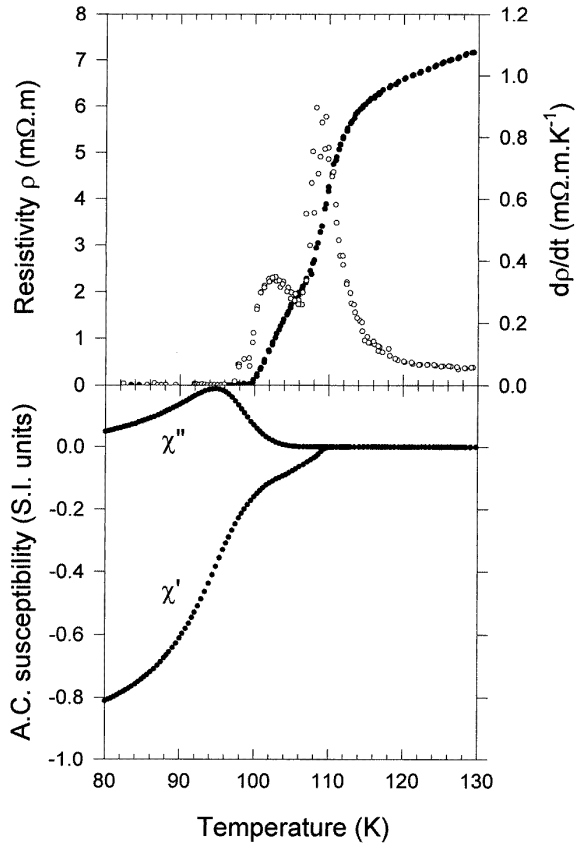

Figure 5: *In-phase and out-of-phase components of the AC susceptibility measured at several AC magnetic fields. From right to left :* B_{AC} *= 0.2, 1, 2, 5, 10, 20 and 50 G. f = 1053 Hz,* B_{DC} *= 0 G.*

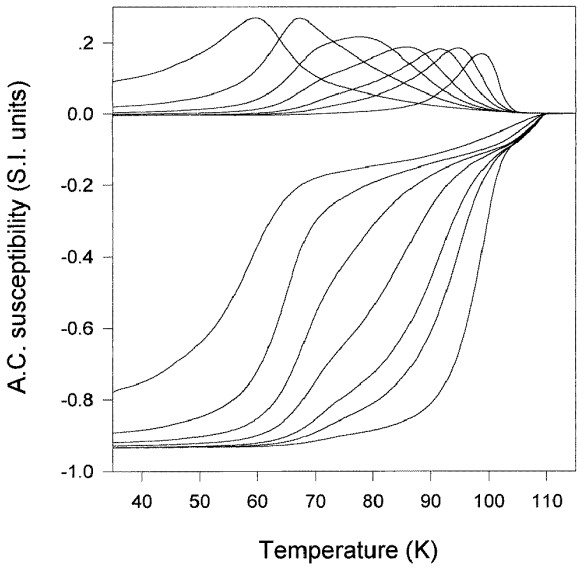

Figure 5 summarizes the AC susceptibility curves measured for different AC magnetic fields, ($\mu_0 h_{AC}$ = 0.2 G-50 G, from right to left). No intragranular peaks are visible, even at high AC fields. The intergranular peak structure is dissymetric. This might be due to the significant proportion of 2212 phase in this material and to weak-link inhomogeneities. This feature also explains the smooth reproducible curvature change for $\chi'(T \approx 75$ K), only visible at low field amplitudes. We have not observed a significant reduction in the peak of χ'' with the

decreasing applied field amplitude. This suggests that reversible fluxoid motion in their potential wells is negligible [6].

Following the Bean model [11], the maximum of the $\chi''(T)$ intergranular peak gives the temperature at which the AC magnetic field approximately coincides with a full flux penetration through the intergranular matrix. This ' B full penetration' versus T curve is given in figure 6. The full-penetration induction B^* is thus 8 G at T = 77 K.

3.2. Critical currents

In order to determine the intergranular-transport critical current at T = 77 K we have used two different procedures. The first one is the AC Campbell-Rollins method [12,13]: a small-ripple AC magnetic field is superimposed onto a large background DC field, here from 20 to 90 G. The critical current density is then deduced from the flux profile gradient, following a generalization of the Bean model in order to take into account the weak link distribution within the sample [14]. The second one is the direct four-point method described previously (section 2.3).

Figure 6: *Full-penetration induction as a function of temperature.*

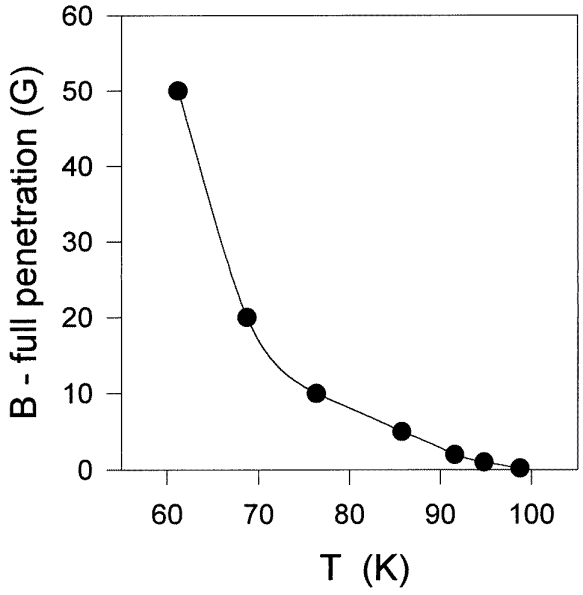

3.2.1. Campbell-Rollins method [12,13].

The volume fraction of diamagnetic grains contained in the sample can be evaluated from the so-called flux profile [12]. Figure 7 exhibits the flux profiles extracted from data measured at f = 1053 Hz according to the Rollins waveform recording procedure [13]. The magnetic field profile reaches its saturation value at p/a = 0.65. The volume fraction f_g of ideal diamagnetic grains contained in the sample is then obtained from $f_g = (1- 0.65)^2 =$ 0.12 [14]. This value is probably lower than the percentage of 2223 phase in the sample since, when p/a = 0.65, magnetic flux is situated in the intergranular matrix and in a layer equal in thickness to the London penetration depth around each grain. Because λ is not negligible with respect to the mean grain radius, the grain proportion is then underestimated.

Following a Bean model generalization [14], the slope of the flux profiles at low field amplitudes is proportional to the intergranular current density J_c. Experimental data (figure 7) clearly show that J_c is strongly affected by the applied DC magnetic field. Because of a wide grain size distribution within the sample (see figure 1), the B_{AC} versus p relationship is quadratic rather than linear and the slope determination is ambiguous. Thus for each curve we have chosen the mean slope in the penetration range 0-0.5 as that giving the J_c value. Results for J_c determination will be discussed in the next section.

Figure 7: *Flux profiles measured at different DC inductions (20-90 G). T = 77 K, f = 1053 Hz. p is the penetration of flux lines and a corresponds to the sample radius.*

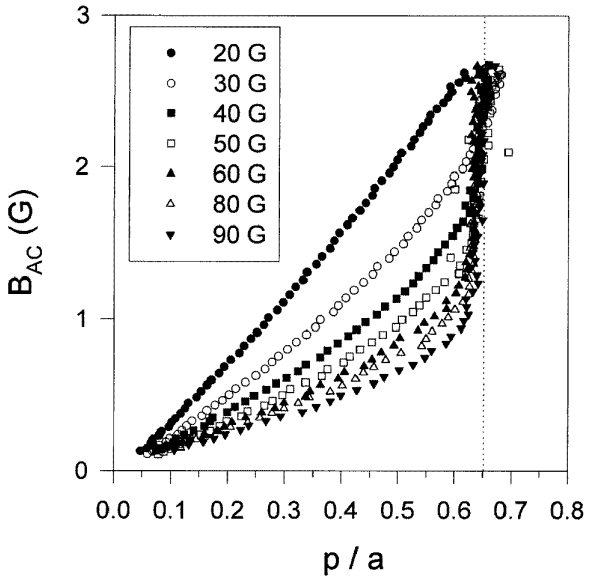

3.2.2. Direct method.

The field dependence of the transport critical current density J_c is plotted in figure 8 and compared with the values deduced from the slope of flux profiles. They are found to be in good agreement with each other. It is of interest in view of much controversy on J_c determination through direct and indirect methods to point out that the agreement is mainly due the following reasons.

(i) J_c is quite low, and then the electrical contact heating effects are unimportant.

(ii) The transport critical current has been determined by applying an external DC magnetic field in such a way that self-field effects are negligible.

(iii) This applied DC magnetic field is much greater than the full-penetration field. In this field range the magnetic flux penetration is nearly frequency independent (cf next section). As a consequence, the different time scales (respectively 50 ms and 1 ms for direct and indirect methods) should not affect the results obtained by using both techniques.

Finally, let us notice that experimental data fit a power law relationship

$$J_C = aB^{-\alpha}$$

with $\alpha = 0.72$. This is in contrast with exponents obtained in [9,10] where values of 0.35 were obtained. Let us recall that a value of 1 is predicted in the 3D Kim model [15], a value of 1/2 for interfacial pinning [16] and a value of 0 for the Bean model. The most general expression with an arbitrary value of the exponent has been considered by Ming *et al* [17]

Figure 8: *Field dependence of the intergranular critical current density at T = 77 K determined by using the direct transport method (●) and deduced from the flux profiles (○). The full line represents the power law fit.*

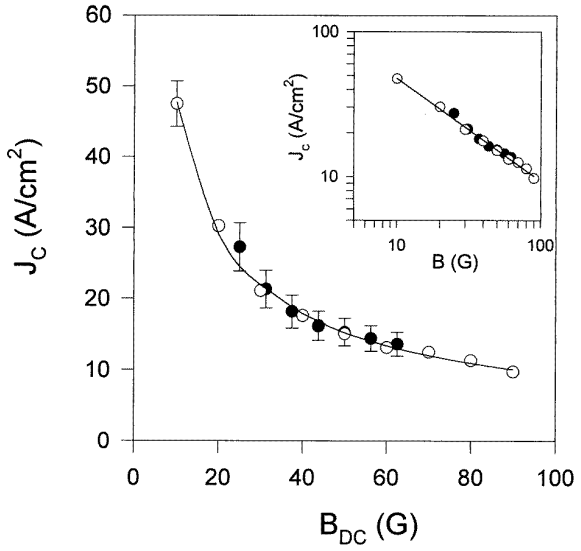

3.3. Flux penetration at zero DC magnetic field

When flux profiles are determined by superimposing a large DC magnetic field onto a small AC magnetic field, the critical current J_c is assumed not to depend on the AC field amplitude. Consequently the variable p calculated by using Campbell formula [12]

$$\frac{p}{a} = 1 - \left(1 - \frac{\mathrm{d}\Phi/\mathrm{d}h}{\mathrm{d}\Phi_N/\mathrm{d}h}\right)^{1/2}$$

(where a denotes the sample radius and Φ_N the in-phase flux in the normal state) represents the flux line penetration depth into the sample. This feature is not true if flux profiles are determined at zero DC field. In this case, the variable p exhibits rather a behaviour characteristic of the $J_c(B)$ dependence [2,18]; p should then be called an 'apparent' penetration depth. Such a profile measured on our BSSCO-2223 ceramics at T = 77 K is displayed in figure 9. At low field amplitudes, p/a increases quasi-linearly with increasing magnetic field. When the field amplitude rises, the apparent penetration depth suddenly decreases to reach a saturation value p/a = 0.65. The angular point occurs for full flux penetration through the intergranular matrix [2]. The deduced full-penetration induction (8 G) and the saturation value (0.65) perfectly corroborate the results obtained in sections 3.1 and 3.2.1.

4. Flux dynamics

Flux creep and thermal activation effects are generally studied by examining the DC magnetization relaxation or the frequency shift of the peak occurring in $\chi''(T)$ [19-21]. Here we have investigated the frequency dependence of the real part of the magnetic susceptibility χ' at T = 77 K.

Results (figure 10) clearly display a logarithmic behaviour between χ' and f. This is characteristic of a thermally assisted flux creep process [19]. This feature suggests that we should consider an activation energy E_a implicitly defined by the equation

$$\chi'(f, B, T) = \chi_0 \left[1 - \frac{kT}{E_a(B,T)} \log\left(\frac{f}{f_0}\right)\right]$$

where k is Boltzmann's constant and f_0 a characteristic frequency. According to different authors [21,22], f_0 generally lies in the range 10^6-10^{13} Hz. A value of $f_0 = 10^{10}$ Hz has been chosen for the fitting of the χ' versus f curves. Values of $E_a(B)$ have been deduced for different AC magnetic inductions (figure 11). A pronounced minimum occurs at B^* = 8 G, which exactly corresponds to the full-penetration induction deduced from the AC

susceptibility curves and the flux profile at zero DC field.

Figure 9: *Flux profile obtained following the Campbell procedure at T = 77 K, f = 1053 Hz and zero DC magnetic field, p is the 'apparent' penetration of flux lines and a corresponds to the sample radius.*

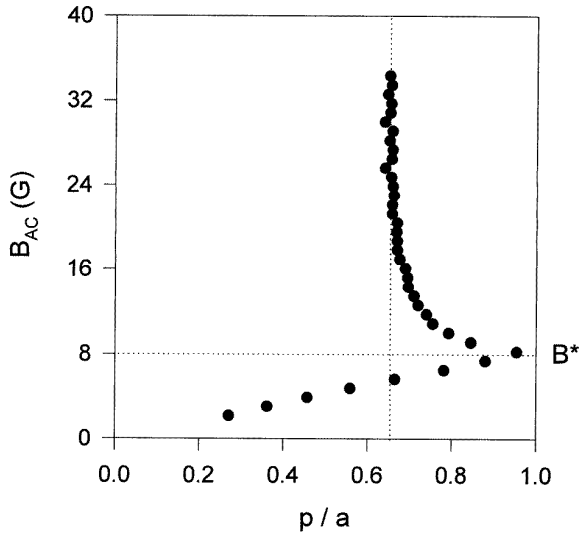

When the applied induction is lower than B^*, the activation energy only refers to Josephson vortices in the intergranular weak-link network. Following theoretical calculations [20], the pinning potential $U(T, H = 0)$ of intergranular vortices in a regular 2D array of Josephson junctions between squared grains is proportional to the maximum Josephson junction current flowing across a grain boundary. However, the relation between the effective activation energy (E_a) and the pinning potential (U) is difficult to establish clearly. One might expect for the activation energy a field dependence behaviour similar to the intergranular current. The power law $B^{-0.72}$ measured previously agrees reasonably with the field dependence of E_a below B^* (straight line in figure 11), although a $(B + B_1)^{-a}$ function should fit experimental data more precisely.

For inductions higher than B^* the measured activation energy rises with increasing magnetic field. This suggests that Abrikosov vortices beginning to penetrate superconducting grains have a higher activation energy than Josephson vortices. Since a greater induction causes a greater Lorentz force acting on flux lines, it is also possible that vortices are depinned and that flux flow effects become predominant with respect to flux creep [20].

5. Conclusions

A set of experimental data has been presented in order to characterize the magnetic behaviour of a polycrystalline BSSCO-2223 sample. AC susceptibility measurements have been compared with electrical resistance data. Intergranular critical current values determined by using a direct transport method and calculated from the flux profile gradient match each other very well. The field dependence of the activation energy has been deduced from a fitting of the χ' versus frequency curves. When the field is lower than the full-penetration field (8 G), the $E_a(B)$ behaviour is found to be similar to that of $J_C(B)$.

Published in: Superconductor Science & Technology (1998), vol.11, iss.1, pp.94-100
Status: Postprint (Author's version)

Figure 10: *(a) In-phase component (χ') of the 77 K AC susceptibility as a function of frequency, measured at several AC magnetic inductions from 0.02 G to 80 G. (b) Vertical expansion of the χ' versus f curve at B = 8 G, showing the logarithmic behaviour.*

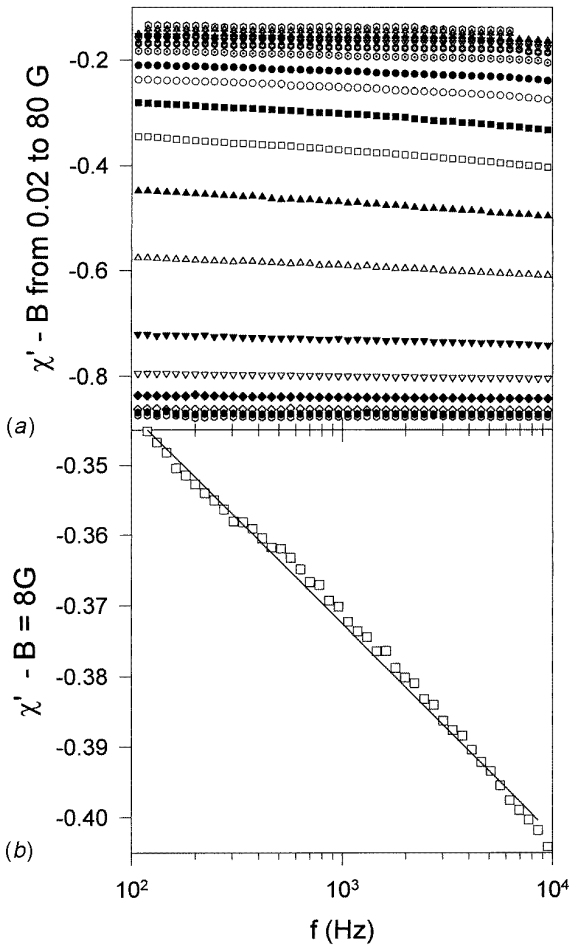

Figure 11: *Activation energy E_a as a function of the AC magnetic induction. Straight line: power law behaviour of $E_a(B)$.*

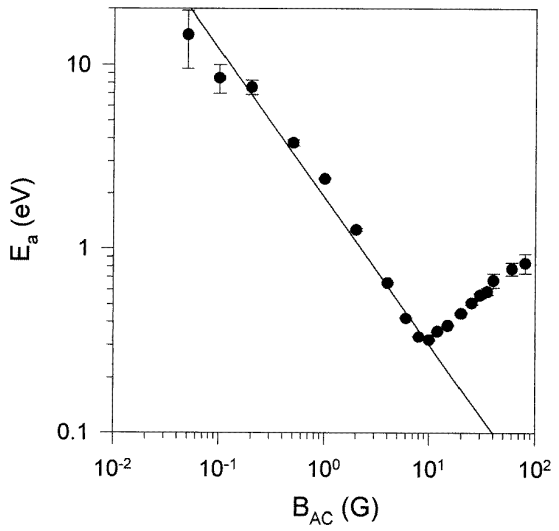

Acknowledgments

PhV is particularly grateful to the FNRS for a research grant. Thanks also go to Professor H W Vanderschueren for its continuing interest and for allowing us access to the MIEL laboratory. This work is part of a ULg 'Action de Recherches Concertées' (ARC 94-99/174).

References

[1] Clem J R 1988 *Physica* C 153-155 50

[2] Campbell A M 1991 *IEEE Trans. Magn.* 27 1660

[3] Campbell A M and Blunt F J 1990 *Supercond Sci. Technol.* 3 450

[4] Frischherz M C, Sauerzopf F M, Weber H W, Murakami M and Emel'chenko G A 1995 *Supercond. Sci. Technol.* 8 485

[5] Otabe E S, Ohtani N, Matsushita T, Ishikawa Y and Yoshizawa S 1994 *Japan. J. Appl. Phys.* 33 996

[6] Matsushita T, Otabe E S and Ni B 1991 *Physica* C 182 95

[7] Ausloos M and Laurent Ch 1988 *Phys. Rev.* B 37 611

[8] Ausloos M, Godelaine P A, Dang A, Hannay C and Cloots R 1991 *Physica* C 185-189 2187

[9] Cloots R, Rulmont A, Godelaine P A, Vanderschueren H W, Bougrine H and Ausloos M 1995 *Europhys. Lett.* 30 487

[10] Cloots R, Dang A, Vanderbemden P, Vanderschueren A, Bougrine H, Vanderschueren H W, Rulmont A and Ausloos M 1996 *Z. Phys.* B 100 551

[11] Bean C P 1964 *Rev. Mod. Phys.* 1 31

[12] Campbell A M 1969 *J. Phys. C: Solid State Phys.* 2 1492

[13] Rollins R W, Küpfer H and Gey W 1974 *J. Appl. Phys.* 45 5392

[14] Godelaine P A and Ausloos M 1990 *Solid. State. Commun.* 76 785

[15] Kim Y B, Hempstead C F and Strnad A R 1962 *Phys. Rev. Lett.* 9 306

[16] Murakami M 1992 *Melt Processed High Temperature Superconductors* ed M Murakami (Singapore: World Scientific)

[17] Ming X, Shi D and Fox R F 1990 *Phys. Rev.* B 42 10773

[18] Campbell A M and Blunt F J 1990 *Physica* C 172 253

[19] Perez F, Obradors X, Fontcuberta J, Bozec X and Fert A 1996 *Supercond. Set Technol.* 9 161

[20] Müller K H, Nikolo M and Driver R 1991 *Phys. Rev.* B 43 7976

[21] Nikolo M and Goldfarb R B 1989 *Phys. Rev.* B 39 6615

[22] Müller K H 1990 *Physica* C 168 585